

REVISED

Conf-941144--96
SAND95-0392C

PERCOLATION MODEL FOR SELECTIVE DISSOLUTION
OF MULTI-COMPONENT GLASSES

RAHUL P. KALE* AND C.J. BRINKER**

*University of New Mexico, Department of Chemical and Nuclear Engineering, Albuquerque, NM 87106

**University of New Mexico, Advanced Materials Laboratory, Albuquerque, NM 87106, and Ceramic Synthesis and Inorganic Chemistry Department 1846, Sandia National Laboratories, Albuquerque, NM 87185.

ABSTRACT

A percolation model is developed which accounts for most known features of the process of porous glass membrane preparation by selective dissolution of multi-component glasses. The model is founded within the framework of the classical percolation theory, wherein the components of a glass are represented by random sites on a suitable lattice. Computer simulation is used to mirror the generation of a porous structure during the dissolution process, reproducing many of the features associated with the phenomenon. Simulation results evaluate the effect of the initial composition of the glass on the kinetics of the leaching process as well as the morphology of the generated porous structure.

The percolation model establishes the porous structure as a percolating cluster of unleachable constituents in the glass. The simulation algorithm incorporates removal of both, the accessible leachable components in the glass as well as the independent clusters of unleachable components not attached to the percolating cluster. The dissolution process thus becomes limited by the conventional site percolation thresholds of the unleachable components (which restricts the formation of the porous network), as well as the leachable components (which restricts the accessibility of the solvating medium into the glass). The simulation results delineate the range of compositional variations for successful porous glass preparation and predict the variation of porosity, surface area, dissolution rates and effluent composition with initial composition and time. For the most part, the results compared well with experimental studies and improved upon similar models attempted in the past.

INTRODUCTION

The group of materials known as controlled pore glasses have long been a subject of interest among researchers especially in recent years. These glasses (of which porous Vycor glass is an example) are characterized by a narrow pore size distribution. They have thus offered practical solutions to many chemical/biological chromatographic problems. They have also been used as a material of choice by researchers to study dynamic and thermodynamic properties of liquids and gases confined to very small spaces (as in a porous network). Interesting examples are studies of super-fluid behavior of ^4He , super-cooling of confined liquids, phase-separation of binary liquid mixtures, water/gas adsorption, etc^{1,2}.

A common technique for making controlled pore glasses is by selective dissolution of glasses³. In this process, the starting material is a multi-component glass where at least one of the constituents is soluble in water or acid. This glass is treated with water to selectively leach out the soluble components giving a porous glass. There are a variety of constituents which are capable of forming glasses suitable for selective dissolution. At least one constituent is

DISTRIBUTION OF THIS DOCUMENT IS UNLIMITED

MASTER

RECEIVED

MAR 15 1995

OSTI

DISCLAIMER

**Portions of this document may be illegible
in electronic image products. Images are
produced from the best available original
document.**

"leachable" and can be any of the metal oxides soluble in water and/or acid other than HF which dissolves silica (e.g. Na_2O , Li_2O , K_2O , B_2O_3). The other component is silica and any of other unleachable metal oxides of group IVB elements of the periodic table (e.g. TiO_2 , SnO_2 , ZrO_2). These components are melted to form a homogeneous glass. Fast cooling of this melt prevents phase separation maintaining a transparent homogeneous glass. Heat treatment of this glass, at temperatures below the melting point, can induce phase separation of the leachable and unleachable components. It is known that both homogeneous and phase separated multicomponent glasses can be leached to give porous, silica rich, substrates⁴.

The final pore size/pore volume/surface area characteristics of the porous glass would depend not only on the degree of phase separation but also on the initial composition of the glass. Other important factors which would play a role in changing the pore specifications would be experimental conditions such as the pH, treatment time, temperature, and inherent diffusional limitations during the dissolution process. Though the structure of the porous glasses have been extensively characterized, little is known about the mechanism of the selective dissolution process. Particularly, a suitable model which would correlate the initial composition of glass, to the rate of leaching and/or the final pore size distribution, is lacking.

PERCOLATION MODEL

Experimental studies on the effect of glass composition on the process of porous glass preparation by selective dissolution have been carried out in the past⁵⁻⁸. By changing the glass composition around some threshold values, large fluctuations in the leach rates of glasses are obtained⁵. Rates of dissolution of sodium borosilicate glasses, as its composition (particularly Si/B ratio) is varied, have been determined⁶. Below a certain critical silica content, all the three constituents (Si, B, and Na) dissolve congruently. The dissolution rates are high and remain constant with respect to time (external diffusional effects were kept to a minimum). When the critical mole fraction of silica is exceeded, Na and B are selectively dissolved, leaving behind a silica rich layer. The dissolution rate decreases rapidly with time. Other researchers have observed that at least a 15% leachable fraction is necessary to form porous glasses^{7,8}.

A percolation model is suggested to explain the above leaching characteristics. The glass network is modeled by a three dimensional regular lattice, with the leachable phase randomly occupying lattice points with a frequency of P_L (representing the fraction of leachable phase in the glass)⁹. This simple representation of the glass structure is a standard site percolation model and known concepts of percolation theory¹⁰ can be applied to explain some of the experimentally observed characteristics of the selective dissolution process. For a very low value of P_L , some sites in the lattice would be occupied by the leachable phase. At higher concentrations, neighboring sites occupied by the leachable phase would form "clusters". With increasing concentration, more and more clusters are formed and their average size keeps increasing. At a critical value of P_L , the largest cluster suddenly spans the whole lattice and becomes an infinite sized cluster. This concentration at which a network of leachable phase percolates through the lattice is termed the "threshold percolation concentration", P_{Lc} , for that lattice. Below the threshold concentration, only finite leachable phase clusters are present in the lattice. Above that concentration, an infinite leachable phase cluster percolates through the lattice along with some finite clusters not yet connected to the backbone network.

Along with the percolating cluster of leachable phase, there also exists an infinite, lattice spanning cluster of the unleachable phase in the lattice. As we increase the fraction of leachable phase, the fraction of unleachable phase in the lattice reduces, and its critical threshold concentration might be reached. Consequently, when the leachable phase concentration reaches P_{Uc} ($=1-P_{Lc}$), the percolating cluster of unleachable phase breaks down into small finite clusters coexisting with the infinite cluster of the leachable phase.

During the leaching processes the surface of the lattice is exposed to a solvating medium. The leachable phase exposed to the solvent is preferentially dissolved, leaving the insoluble

components intact. The solvent can enter through the pores formed to further leach out the accessible leachable components of the glass and create a porous network. Below the percolation threshold of the leachable phase, P_{LC} , there is no accessible continuous network of soluble components for the dissolution path to follow. The aqueous phase will not be able to penetrate far into the glass and only surface clusters of the leachable phase would be dissolved.

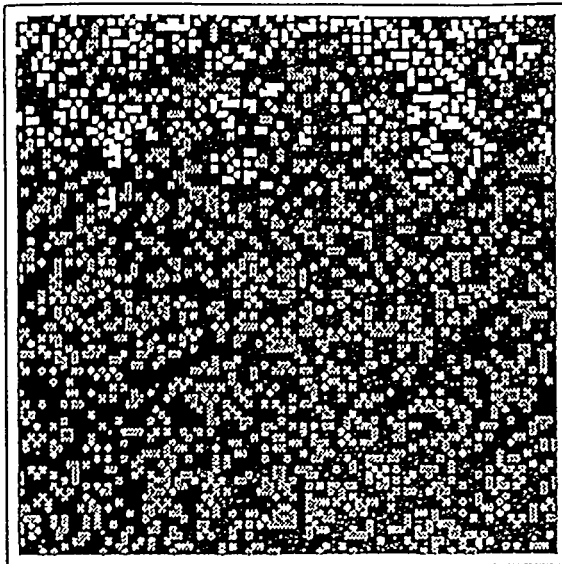
Above the critical concentration P_{LC} , the leachable phase would release into the solvent along with the finite clusters of the unleachable components. The infinite lattice spanning cluster of the unleachable phase would remain on the parent glass and hinder the transport of glass constituents from the dissolution front to the bulk aqueous phase. This diffusional limitation would cause the dissolution rates to decrease with time. Further, if P_L is increased beyond the threshold value of P_{UC} , the dissolution of leachable components would necessitate the release of all finite unleachable phase clusters. Due to the absence of an infinite insoluble cluster, nothing would be left on the glass substrate and the dissolution front would remain essentially flat. No porous silica framework can form and there is no diffusional limitation for product removal. Consequently the rate of leaching is expected to be much higher and also to remain constant.

Successful porous glass formation would thus occur only if the leachable fraction lies within the range of P_{LC} and P_{UC} . Below P_{LC} , the solvating medium would not be able to penetrate the glass, and above P_{UC} , a continuous network of unleachable phase does not exist. The above percolation model thus adequately explains some experimentally observed facts, especially the sharp transition in the leaching rate characteristics across certain threshold concentration, P_{LC} and P_{UC} .

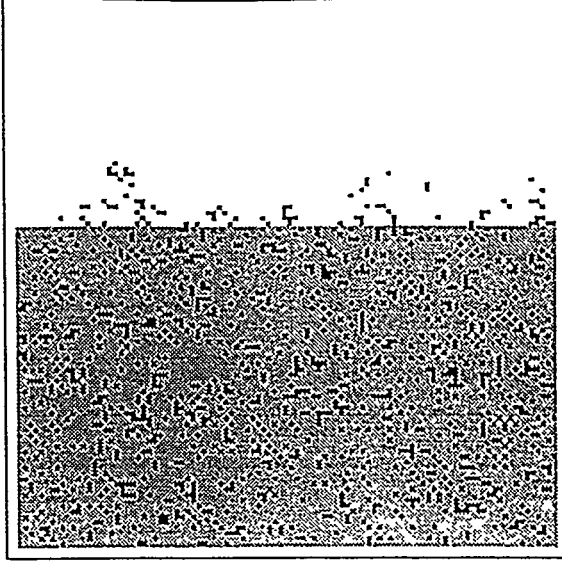
COMPUTER SIMULATIONS

An algorithm was developed which simulates the dissolution process by dissolving out, at each time step, the accessible leachable phase along with any new independent clusters of the unleachable phase formed just behind the dissolution front. The continuous random covalent network structure of glass is ideally represented by the Voronoi random network. However, the simulation calculations can be simplified by using a body centered cubic lattice with second nearest neighbor bonding (BCC2) which gives a close approximation to the Voronoi network¹¹. The coordination number for this lattice is 14 and the threshold percolation concentration is 0.17. A 100X100X100 body centered cubic lattice was used for the simulations.

To model the initial glass structure before the dissolution step, sites in the lattice are randomly occupied by leachable phase species with a probability of the desired leachable fraction. The remaining sites are assumed to be occupied by the unleachable phase. Each site then has 14 nearest neighbors. Since the lattice is finite, the boundary conditions of the lattice has to be defined. Periodic boundary conditions are used such that the neighbors of the sites on the faces of the cube are the sites on the opposite faces. This condition is used for the four sides of the cube. The upper neighbors of the top face are set to be occupied by voids and the lower neighbors of the bottom face are set to be occupied by leachable phase atoms. This lattice then simulates a thin glass membrane of infinite size where the top surface is exposed to a solvent. To simulate the selective dissolution process, the lattice is repeatedly scanned for sites occupied by leachable phase atoms, and their nearest neighbor configuration is determined. If any site has at least one nearest neighbor as a void, the occupancy of that site is changed from the leachable phase atom to a void. Each scan of the lattice becomes equivalent to a time step of the dissolution process. After each of these scans, all unleachable phase clusters completely surrounded by voids are located and these sites are also converted to voids. This is achieved by calculating the sizes of all clusters assuming that both leachable and unleachable atoms belong to one phase and all the voids belong to the other phase. The largest cluster then represents the unattacked substrate and all smaller clusters are free clusters of the unleachable phase. The sizes of the clusters are evaluated by using a technique based on an efficient cluster counting algorithm first proposed by Hoshen and Kopelman (1976)¹². The scanning and free cluster dissolving process is repeated until no leachable phase atoms are found with void nearest neighbors.



(a)



(b)

Fig.1 The dissolution front is represented by a vertical cross-sectional slice of the lattice. The site occupancy after 40 iterations of the simulation are shown for (a) $P_L = 0.25$ and (b) $P_L = 0.85$

SIMULATION RESULTS AND DISCUSSION

To visualize dissolution fronts in the body-centered cubic lattice, cross-sectional slices of the lattice were examined. The sites occupied by the unleachable phase, leachable phase, and the pores were represented by black, gray and white squares respectively. Typical plots for $P=0.25$ and 0.85 are shown in Fig 1. In cases where P_L was less than P_{Lc} , the formation of voids was restricted to a few surface clusters only. In Fig 1(a), where the leachable phase concentration is more than P_{Lc} , an infinite cluster can be seen on the surface. The grays turn to whites as the dissolution front travels downwards. The figures were plotted when the simulation runs reached a time step of 40. Some gray sites of the leachable phase that are inaccessible have not been dissolved out and can be seen totally surrounded by black squares. Though it is not evident from the figure, all finite clusters of the unleachable phase have been dissolved out. In Fig 1(b) where $P_L > P_{Lc}$, the release of finite clusters of the unleachable phase produces a dissolution front which is essentially flat and no parent cluster is left on the surface. The free hanging black squares in Fig. 1(b) are actually connected to the main cluster through slices not in the plane of the paper.

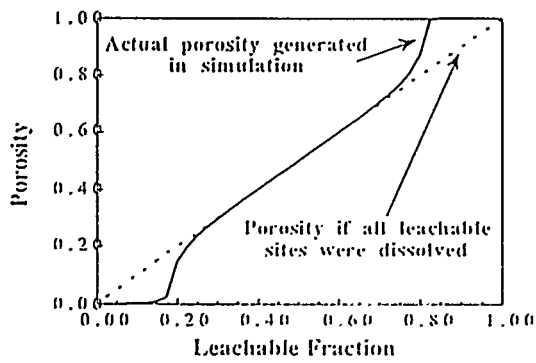


Fig. 2 Porosity vs initial leachable phase concentration

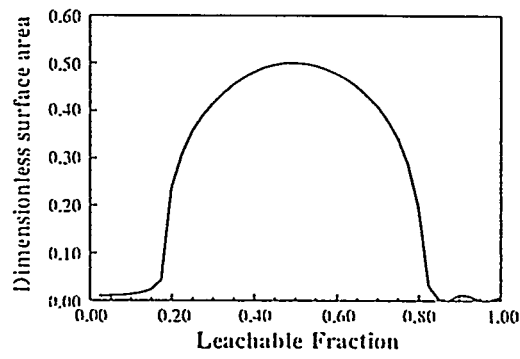


Fig. 3 Dimensionless surface area vs initial leachable phase concentration

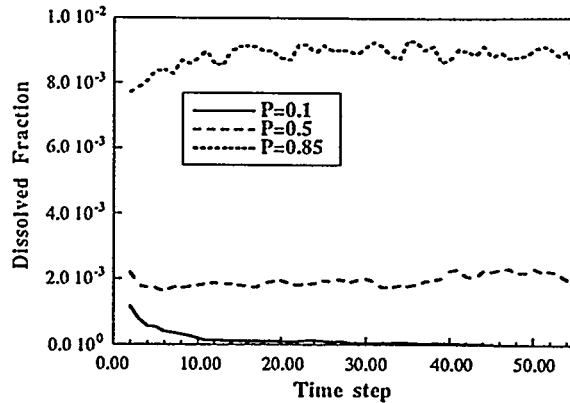


Fig. 4 Fraction of dissolved sites vs. time for three different initial concentrations

The total achieved porosity is calculated as the ratio of total number of sites occupied by voids after complete dissolution to the total number of sites in the lattice. This is plotted versus the initial leachable phase concentration in Fig. 2. Each data point (totally 40 points, not shown) corresponds to a simulation run at a given initial fraction of the leachable phase. It is seen that significant porosity starts getting generated only above the percolation threshold and does not reach the leachable fraction until about 0.30. Above the concentration of around 0.8, the achieved porosity suddenly shoots up to almost 100% meaning that the lattice is essentially empty and no porous structure has been generated.

A dimensionless surface area is calculated as the ratio of total number of nearest neighbor bonds between voids and solid substrate in the lattice to the total number of such bonds possible in the lattice. The dimensionless surface area generated after complete dissolution as a function of the leachable fraction is plotted in Fig. 3. As expected, negligible total surface area is achieved above and below P_{Uc} and P_{Lc} . Maximum normalized surface area is seen at a leachable fraction of 0.5. The actual surface area can be related to the dimensionless surface area if the pore size is known. If the pore size is d_p and the dimensionless surface area is ϕ then the actual surface area per unit volume is evaluated as $3\phi/d_p$.

The rates of dissolution can be represented by plotting the fraction of total number of sites turning into voids during each time step as a function of time. Typical plots for three different initial concentrations are shown in Fig. 4. For a leachable fraction less than the percolation threshold P_{Lc} , the rate of dissolution falls rapidly to zero as the solvent is not able to penetrate into the substrate. For glasses with leachable fraction greater than the threshold, the rate of dissolution remains approximately constant with time till almost all of the unleachable phase is dissolved out. Since diffusional limitations for product removal were not considered in the simulations, the characteristic decrease in dissolution rate for initial leachable fractions between P_{Lc} and P_{Uc} is not evident in the plot (Fig. 4, $P_L = 0.5$).

Experimentally determined⁶ values of the parameter γ , defined as the ratio of fraction of unleachable phase in the leached effluent to that in the original glass is plotted in Fig. 5. Since all components in the glass dissolve at the same time above the threshold concentration of the unleachable phase, the mole fraction of all ions in the leached effluent would be the same as in the original glass. Consequently, the ratio γ in Fig. 5 shows a sharp jump from near zero values to unity at a particular glass composition (around 57% leachables). Values of γ evaluated during the simulations, are plotted in Fig. 6. Though the characteristic jump is seen in both the plots, its location does not coincide. The early breakdown of porous network in the laboratory could be attributed to the decrease in mechanical strength of the infinite cluster which becomes more and more tenuous as the leachable phase concentration is increased and the threshold concentration of unleachable phase is approached. The developing porous structure cannot withstand the high degree of mechanical agitation maintained during the experiments and congruent dissolution of

the glass components is seen well below the expected concentration of 0.83. It is also possible that the percolation thresholds of the lattice may shift due to structural rearrangement of the glass constituents such as during phase separation.

CONCLUDING REMARKS

The mechanics of selective dissolution process for porous glass formation can be explained very well by using concepts of the percolation theory. Trends in experimental behavior as observed by various workers can be understood by simulating the random network structure of glasses by a site percolation model on a BCC2 lattice. Particularly the upper and lower bounds for the leachable fraction in the multicomponent glasses are clearly delineated.

Inclusion of diffusional limitations in the dissolution simulations could be an interesting task for the future. Also, percolation concepts could be used for cases where there are more than two components, each phase having a different solubility.

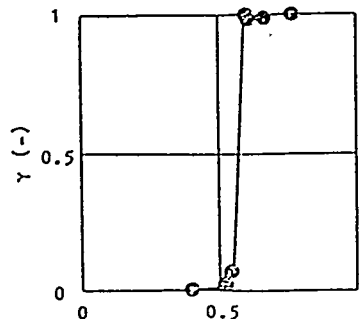


Fig.5 Experimental gamma vs. initial leachable phase concentration
[reprinted from Ref. 6]

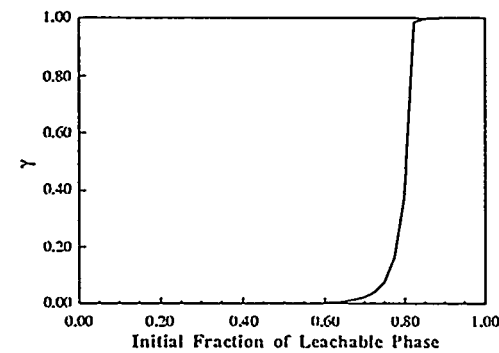


Fig.6 Computed Gamma vs initial leachable phase Concentration

ACKNOWLEDGEMENTS

The authors would like to thank, NSF, Gas Research Institute, Electric Power Research Institute, and Morgantown Energy Technology Center for funding this research.

Sandia National Laboratories is a U.S. Department of Energy Facility supported by DOE Contract No. DE.AC04.76.DP00789.

REFERENCES

1. G.S. Iannacchione, G.P. Crawford, S. Zumer, J.W. Doane, and D. Finotello, *Physical Review Letters*, 71, 2595 (1993).
2. P. Levitz, G. Ehret, S.K. Sinha, and J.M. Drake, *J. Chem. Phys.*, 95, 6151 (1991).
3. H.P. Hood and M.E. Nordberg, U.S. Patent No. 2,286,275 (1942).
4. L. Holland, *The Properties of Glass Surfaces*, (London Chapman and Hall, 1966), p. 181.
5. X. Feng, I.L. Pegg, A. Barkatt, P.B. Macedo, S.J. Cucinell, and S. Lai, *Nucl. Technol.*, 85, 334 (1989).
6. M. Kinoshita, M. Harada, Y. Sato, and Y. Hariguchi, *J. Am. Ceram. Soc.*, 74, 783 (1991).

7. J.J. Hammel, The Journal of Chemical Physics, **46**, 2234 (1967).
8. J.J. Hammel, U.S. Patent No. 4,853,001 (1989).
9. A.B. Shelekhin, A.G. Dixon, and Y.H. Ma, J. of Membrane Science, **83**, 181 (1993).
10. R Zallen, The Physics of Amorphous Solids, (Wiley-Science Publications, New York, 1983).
11. G.R. Jerauld, L.E. Scriven, and H.T. Davis, J. Phys. C: Solid State Phys., **17**, 3429 (1984).
12. J. Hoshen, and R. Kopelman, Physical Review B., **14**, 3438 (1976).

This work was supported by the DOE on contract number DE-AC04-94AL85000 at Sandia National Laboratories

DISCLAIMER

This report was prepared as an account of work sponsored by an agency of the United States Government. Neither the United States Government nor any agency thereof, nor any of their employees, makes any warranty, express or implied, or assumes any legal liability or responsibility for the accuracy, completeness, or usefulness of any information, apparatus, product, or process disclosed, or represents that its use would not infringe privately owned rights. Reference herein to any specific commercial product, process, or service by trade name, trademark, manufacturer, or otherwise does not necessarily constitute or imply its endorsement, recommendation, or favoring by the United States Government or any agency thereof. The views and opinions of authors expressed herein do not necessarily state or reflect those of the United States Government or any agency thereof.